Electronic Supplementary Material (ESI) for Dalton Transactions.
This journal is © The Royal Society of Chemistry 2020

Supporting InformationQ

Ultrafine NiFe Clusters Anchored on N-Doped Carbon as Bifunctional Electrocatalysts for Efficient Water and Urea Oxidation

Jingfang Zhang,[a,] Fei Xing,[a] Hongjuan Zhang,[a] and Yi Huang[b,*]*

[a] Department of Chemistry, College of Science, Hebei Agricultural University, Baoding 071001, China; E-mail: zjf1991211@163.com

[b] Department of Chemistry, School of Science, Tianjin University, Tianjin 300072, China; E-mail: yihuang@tju.edu.cn

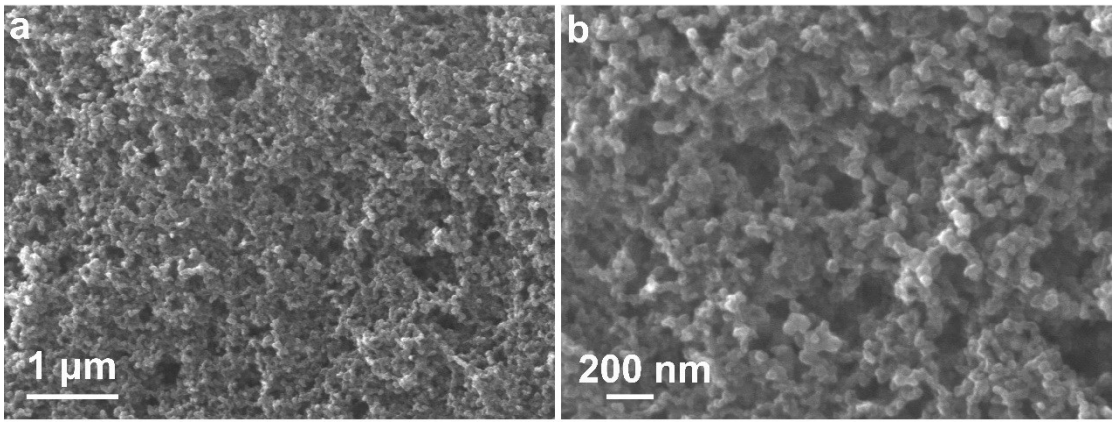

Figure S1. Low-resolution (a) and high-resolution (b) SEM images of commercial Ketjenblack.

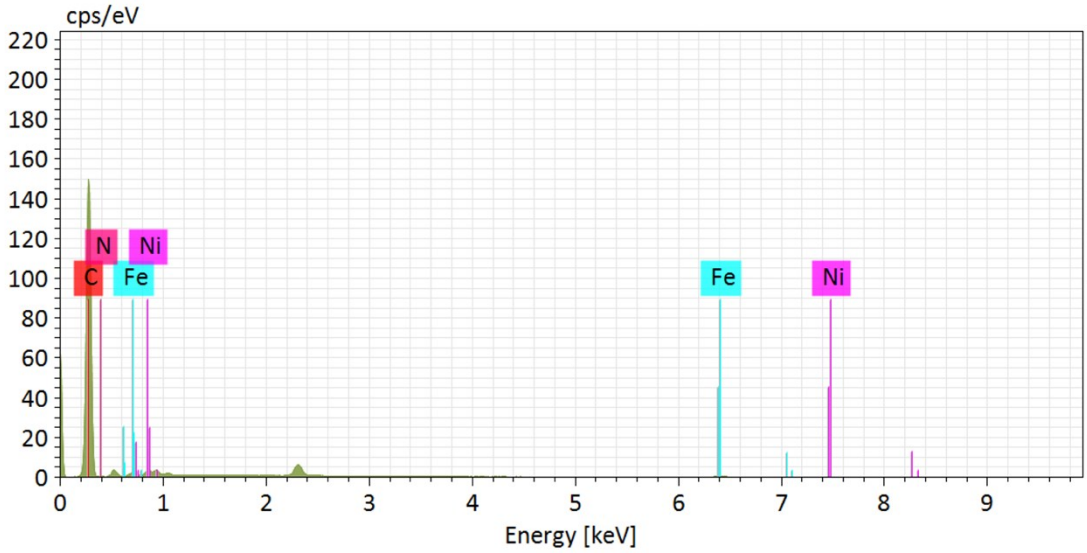

Figure S2. EDS spectrum of NiFe/N-C.

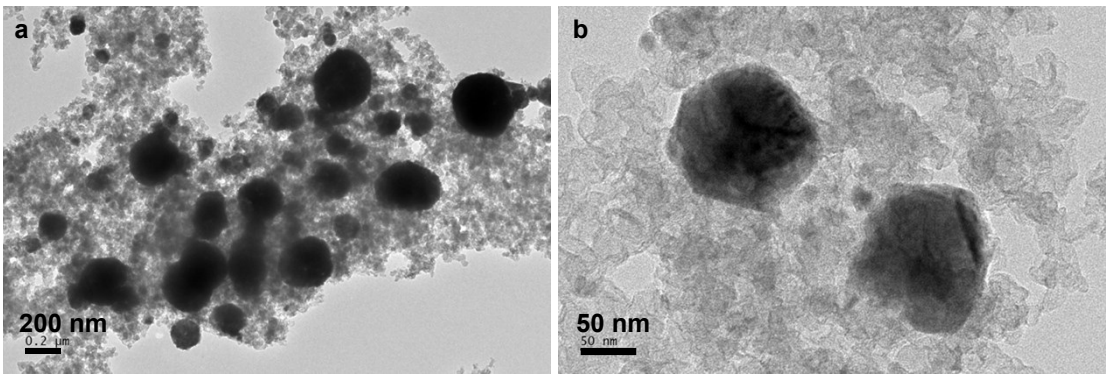

Figure S3. Low-resolution (a) and high-resolution (b) TEM images of NiFe/C.

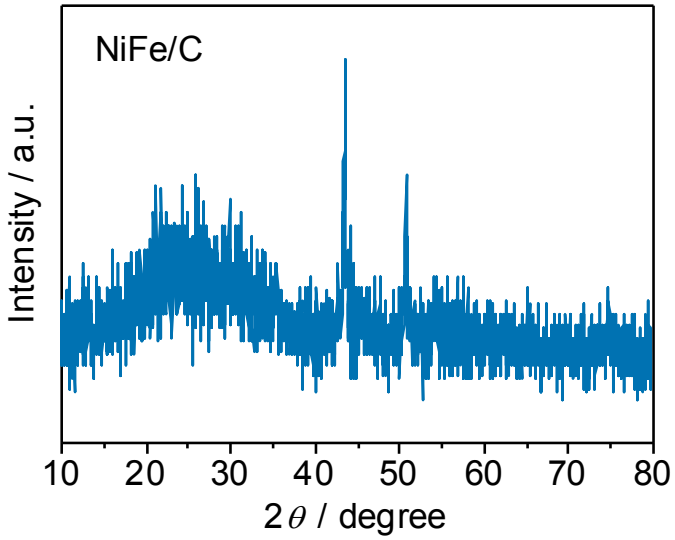

Figure S4. XRD pattern of NiFe/C.

Figure S5. Optical photograph of NiFe/N-C with gram-scale synthesis.

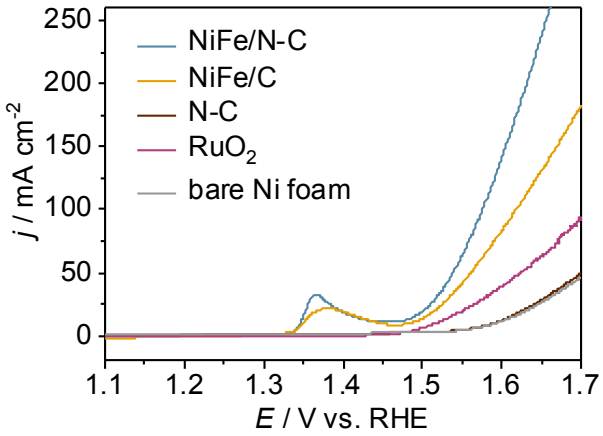

Figure S6. LSV curves (without iR correction) for NiFe/N-C, NiFe/C, N-C, RuO_2, and bare Ni foam toward OER.

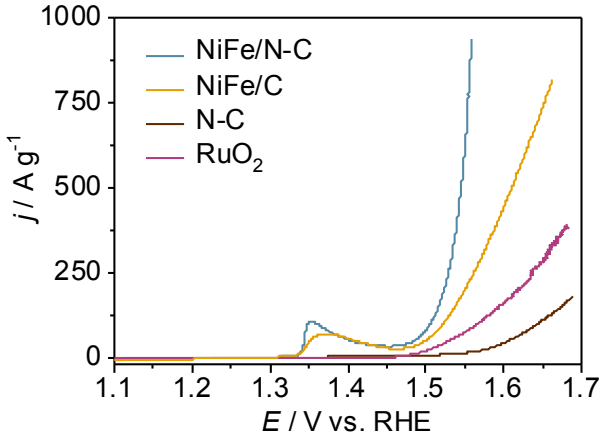

Figure S7. Mass activity of NiFe/N-C, NiFe/C, N-C, and RuO_2 toward OER.

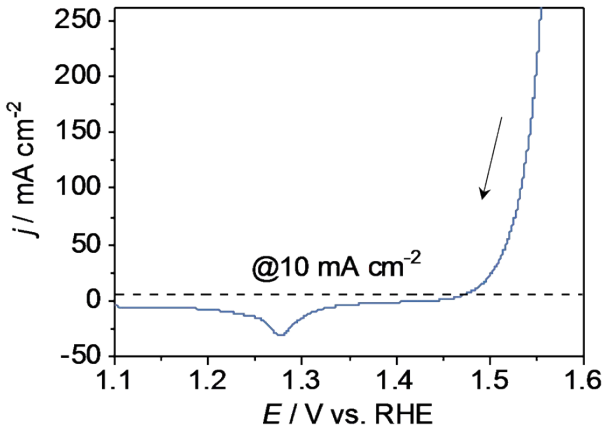

Figure S8. The LSV curve of NiFe/N-C performed from the positive to the negative direction.

To avoid the overlap of the oxidation peak with the OER onset currents, we scanned the voltage from the positive to the negative direction (Figure S8) and determine that the NiFe/N-C only needs an overpotential of 250 mV to reach 10 mA cm^{-2}.

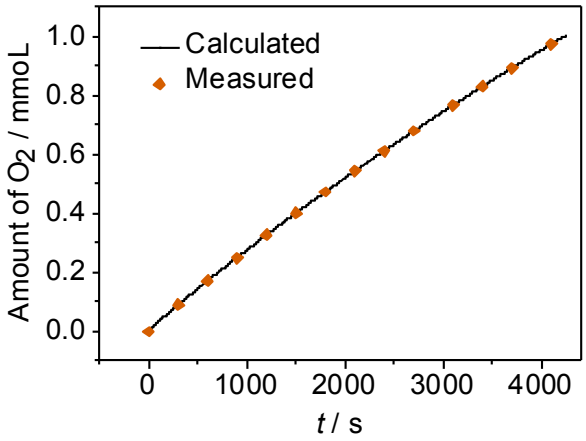

Figure S9. The amount of evolved oxygen theoretically calculated and experimentally measured versus time for NiFe/N-C over the course of OER.

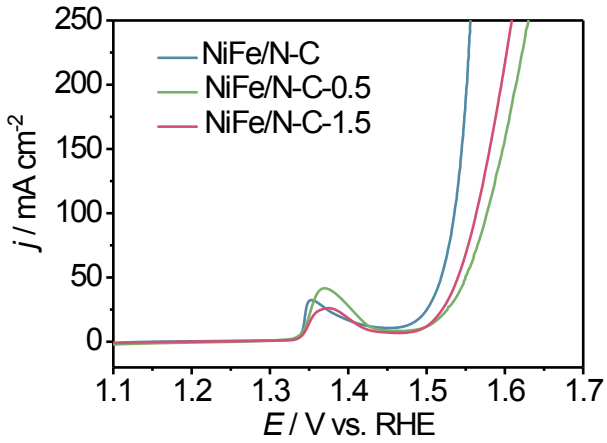

Figure S10. LSV curves of NiFe/N-C with different mole ratio of Ni and Fe.

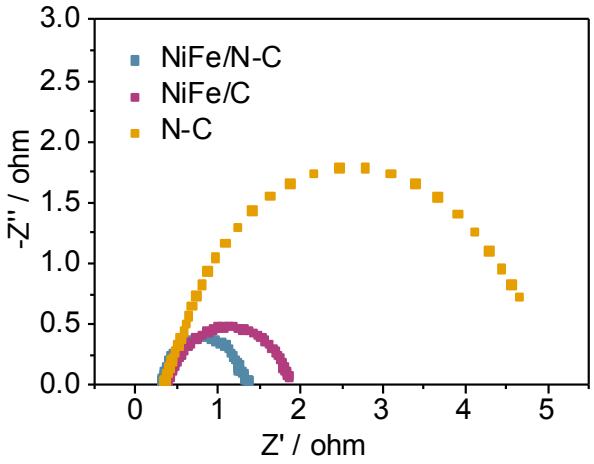

Figure S11. The Nyquist plots of NiFe/N-C, NiFe/C and N-C catalysts under a potential of 1.52 V vs. RHE.

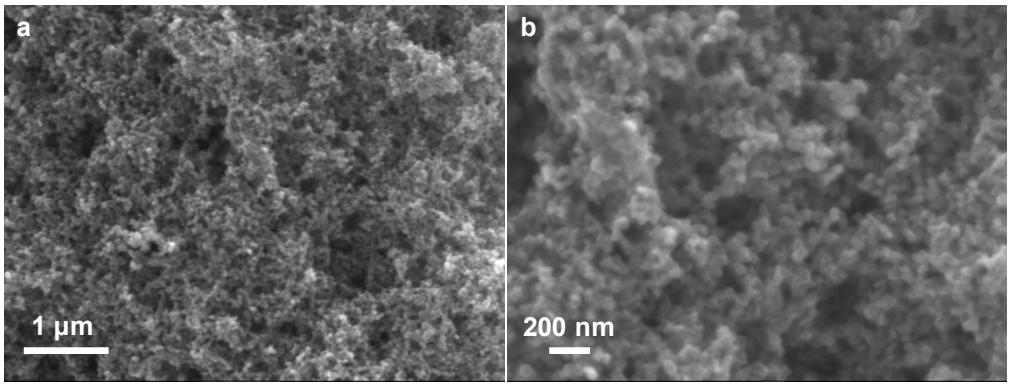

Figure S12. Low-resolution (a) and high-resolution (b) SEM images of NiFe/N-C after electrocatalytic measurements.

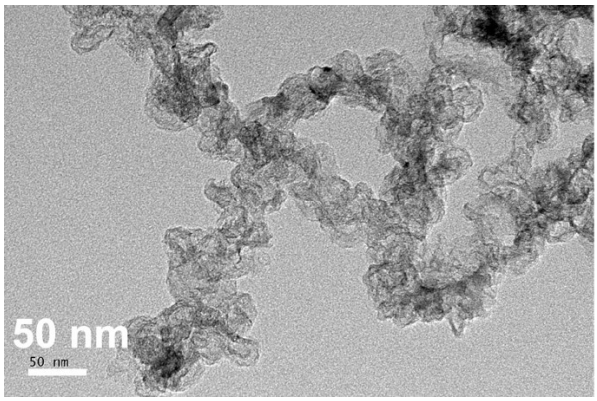

Figure S13. TEM image of NiFe/N-C after electrocatalytic measurements.

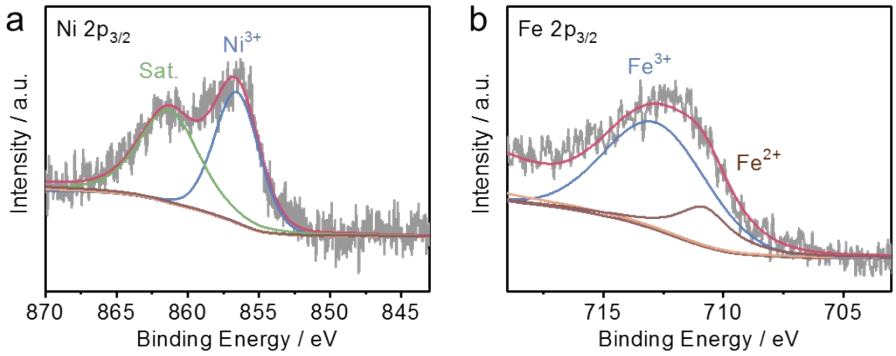

Figure S14. (a) Ni $2p_{3/2}$, and (b) Fe $2p_{3/2}$ high-resolution XPS spectra for the NiFe/N-C after electrochemical measurements.

Figure S14 shows the peaks of Ni^{3+} and $Fe^{2+/3+}$, and peaks corresponding to metallic Ni and Fe are not observed, suggesting metal (oxy)hydroxides appears during electrooxidation conditions, which is consistent with the conclusion that ultrasmall Ni-based nanoparticles (sub-10 nm) could undertake deep reconstruction by electro-oxidation reported by Liu *et al.*.[15] These results suggest that the

oxidized species may act as the actual active site for the electrooxidation reaction, as observed for most electrooxidation catalysts. [16-18]

Table S1. Comparisons of OER performances among NiFe/N-C and other metal-carbon hybrid electrocatalysts in the literatures.

Materials	Electrolyte	Overpotential (mV)	Current density (mA cm^{-2})	Tafel slope (mV dec^{-1})	Mass loading (mg cm^{-2})	Reference
NiFe/N-C	1 M KOH	260 250	20 10	42	0.304	This work
NiFe/N-CNT	0.1 M KOH	290	10	79	0.4	[1]
HCM@Ni-N	1 M KOH	304	10	76	1.52	[2]
FeNi@NC	1 M NaOH	310	20	70	0.32	[3]
NiFe/CN_x	0.1 M KOH	360	10	59	0.514	[4]
FeCoNi@G	1 M KOH	288	10	60	0.32	[5]
FeNi@NC-NG	1 M KOH	270	10	72	0.5	[6]

NiFe@C	1 M KOH	281	10	53	0.286	[7]
Co−N−C	1 M KOH	321	10	40	0.38	[8]
Co@C	1 M KOH	333	10	58	0.04	[9]

Table S2. Comparisons of UOR performances among NiFe/N-C and Ni(Fe)-based electrocatalysts in the literatures.

Materials	Potential (V)	Current density (mA cm^{-2})	Mass loading (mg cm^{-2})	Reference
NiFe/N-C	1.37	100	0.304	This work
$Ni(OH)_2$	~1.58	100	0.285	[10]
$NiFe_2O_4$	1.361	10	0.2	[11]
NiFe LDH	1.459	100	—	[12]
$Ni_2P/Ni_{0.96}S$	1.441	100	1.33	[13]
NiMoO-Ar	1.42	100	5.1	[14]

Reference

[1] Lei H, Wang Z, Yang F*, et al.* NiFe nanoparticles embedded N-doped carbon nanotubes as high-efficient electrocatalysts for wearable solid-state Zn-air batteries. Nano Energy, 2019, 68: 104293

[2] Zhang H, Liu Y, Chen T*, et al.* Unveiling the Activity Origin of Electrocatalytic Oxygen Evolution over Isolated Ni Atoms Supported on a N-Doped Carbon Matrix. Adv Mater, 2019, 31: e1904548

[3] Cui X, Ren P, Deng D, Deng J, Bao X. Single layer graphene encapsulating non-precious metals as high-performance electrocatalysts for water oxidation. Energ Environ Sci, 2016, 9: 123-129

[4] Ci S, Mao S, Hou Y*, et al.* Rational design of mesoporous NiFe-alloy-based hybrids for oxygen conversion electrocatalysis. J Mater Chem A, 2015, 3: 7986-7993

[5] Yang Y, Lin Z, Gao S*, et al.* Tuning Electronic Structures of Nonprecious Ternary Alloys Encapsulated in Graphene Layers for Optimizing Overall Water Splitting Activity. ACS Catal, 2016, 7: 469-479

[6] Zhang X, Li C, Si T*, et al.* FeNi Cubic Cage@N-Doped Carbon Coupled with N-Doped Graphene toward Efficient Electrochemical Water Oxidation. ACS Sustain Chem Eng, 2018, 6: 8266-8273

[7] Feng Y, Yu X Y, Paik U. N-doped graphene layers encapsulated NiFe alloy nanoparticles derived from MOFs with superior electrochemical performance for oxygen evolution reaction.

Sci Rep, 2016, 6: 34004

[8] Bai L, Hsu C S, Alexander D T L, Chen H M, Hu X. A Cobalt-Iron Double-Atom Catalyst for the Oxygen Evolution Reaction. J Am Chem Soc, 2019, 141: 14190-14199

[9] Xiao Q, Zhang Y, Guo X*, et al.* A high-performance electrocatalyst for oxygen evolution reactions based on electrochemical post-treatment of ultrathin carbon layer coated cobalt nanoparticles. Chem Commun, 2014, 50: 13019-13022

[10] Yang W, Yang X, Li B*, et al.* Ultrathin nickel hydroxide nanosheets with a porous structure for efficient electrocatalytic urea oxidation. J Mater Chem A, 2019, 7: 26364-26370

[11] Wu F, Ou G, Wang Y*, et al.* Defective $NiFe_2O_4$ Nanoparticles for Efficient Urea Electrooxidation. Chem Asian J, 2019, 14: 2796-2801

[12] Xie J, Qu H, Lei F*, et al.* Partially Amorphous Nickel-Iron Layered Double Hydroxide Nanosheet Arrays for Robust Bifunctional Electrocatalysis. J Mater Chem A, 2018, 6: 16121-16129

[13] He M, Feng C, Liao T*, et al.* Low-Cost $Ni_2P/Ni_{0.96}S$ Heterostructured Bifunctional Electrocatalyst toward Highly Efficient Overall Urea-Water Electrolysis. ACS Appl Mater Interfaces, 2020, 12: 2225-2233

[14] Yu Z-Y, Lang C-C, Gao M-R*, et al.* Ni–Mo–O nanorod-derived composite catalysts for efficient alkaline water-to-hydrogen conversion via urea electrolysis. Energ Environ Sci, 2018, 11: 1890-1897

[15] Liu X, Ni K, Wen B, *et al.* Deep Reconstruction of Nickel-Based Precatalysts for Water Oxidation Catalysis. ACS Energy Lett, 2019, 4: 2585-2592

[16] Xu K, Ding H, Lv H*, et al.* Dual Electrical-Behavior Regulation on Electrocatalysts Realizing Enhanced Electrochemical Water Oxidation. Adv Mater, 2016, 28: 3326-3332

[17] Chen P, Xu K, Fang Z*, et al.* Metallic Co_4N Porous Nanowire Arrays Activated by Surface Oxidation as Electrocatalysts for the Oxygen Evolution Reaction. Angew Chem Int Ed, 2015, 54: 14710-14714

[18] Ji L, Wang J, Teng X, Meyer T J, Chen Z. CoP Nanoframes as Bifunctional Electrocatalysts for Efficient Overall Water Splitting. ACS Catal, 2020, 10: 412-419